01 Jul 2019

The Blue Emission at 2.8 EV in Strontium Titanate: Evidence for a Radiative Transition of Self-Trapped Excitons from Unbound States

Miguel L. Crespillo

Joseph T. Graham
Missouri University of Science and Technology, grahamjose@mst.edu

Fernando Agullo-Lopez

Y. Zhang

et. al. For a complete list of authors, see https://scholarsmine.mst.edu/nuclear_facwork/469

Recommended Citation

M. L. Crespillo et al., "The Blue Emission at 2.8 EV in Strontium Titanate: Evidence for a Radiative Transition of Self-Trapped Excitons from Unbound States," *Materials Research Letters*, vol. 7, no. 7, pp. 298-303, Taylor & Francis Ltd., Jul 2019.
The definitive version is available at https://doi.org/10.1080/21663831.2019.1604444

MATER. RES. LETT.
2019, VOL. 7, NO. 7, 298–303
https://doi.org/10.1080/21663831.2019.1604444

MATERIALS RESEARCH LETTERS
Taylor & Francis
Taylor & Francis Group

ORIGINAL REPORT

The blue emission at 2.8 eV in strontium titanate: evidence for a radiative transition of self-trapped excitons from unbound states

M. L. Crespillo [a], J. T. Graham[a,b], F. Agulló-López[c], Y. Zhang [d] and W. J. Weber [a,d]

[a]Department of Materials Science and Engineering, University of Tennessee, Knoxville, TN, USA; [b]Department of Mining and Nuclear Engineering, Missouri University of Science and Technology, Rolla, Missouri, USA; [c]Centro de Microanálisis de Materiales, CMAM-UAM, Cantoblanco, Madrid, Spain; [d]Materials Science and Technology Division, Oak Ridge National Laboratory, Oak Ridge, TN, USA

ABSTRACT

The origin of the blue emission in $SrTiO_3$ has been investigated as a function of irradiation fluence, electronic excitation density, and temperature using a range of ion energies and masses. The emission clearly does not show correlation with the concentration of vacancies generated by irradiation but is greatly enhanced under heavy-ion irradiation. The intensity ratio of the 2.8 and 2.5 eV bands is independent of fluence at all temperatures, but it increases with excitation rate. The 2.8 eV emission is proposed to correspond to a transition from conduction band states to the ground state level of the self-trapped exciton center.

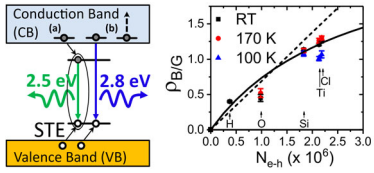

IMPACT STATEMENT

A novel mechanism attributes the origin of the intriguing blue band in $SrTiO_3$ to a non-localized transition of the self-trapped exciton center from conduction band states to the ground level.

ARTICLE HISTORY
Received 22 January 2019

KEYWORDS
$SrTiO_3$; electronic excitation density; self-trapped excitons; oxygen vacancies; ionoluminescence

1. Introduction

Strontium titanate ($SrTiO_3$) is a model transition metal oxide, receiving intensive attention due to its many applications. This multifunctional perovskite ceramic has remarkable physical and chemical properties, including high temperature superconductivity, photocatalytic behavior and 'colossal' magnetoresistance [1–4]. It is often considered to constitute the basis for oxide-based microelectronics [5]. The electronic and optical behavior is presently an active and controversial field of research [6–9]. The luminescence spectra under a variety of excitation sources, including UV light [8–18], X-rays [19], electrons [20] and ion-beams [21,22], show three main bands centered at 2.0 eV (red), 2.5 eV (green) and 2.8 eV (blue). A detailed study using ion-beam irradiation experiments has concluded that the red band is due to *d-d* transitions between an excited level in the conduction band (CB) with mostly $3d(t_{2g})$ character and an *in-gap* $3d(e_g)$ level associated with an electron self-trapped as Ti^{3+} adjacent to an oxygen vacancy (Ti^{3+}-V_O center) [23–28], as illustrated in Figure S1 (see supplementary data online). It is generally accepted that the green 2.5 eV emission band is associated with a triplet–singlet optical transition of a self-trapped exciton (STE) [8,9,19,29]. The situation for the 2.8 eV band is more controversial. A number of proposals on the origin of this emission have been advanced, including its relationship with oxygen vacancies [9–11]. Several authors [11,12,17] have proposed that the blue band may be associated with a transition from the conduction band minimum (CBM) to the *in-gap* level of a self-trapped hole (STH) [30]; whereas others [6] suggest a transition from

CONTACT M. L. Crespillo mcrespil@utk.edu Department of Materials Science and Engineering, University of Tennessee, Knoxville, TN 37996, USA; W. J. Weber wjweber@utk.edu Department of Materials Science and Engineering, University of Tennessee, Knoxville, TN 37996, USA; Materials Science and Technology Division, Oak Ridge National Laboratory, Oak Ridge, TN 37831, USA

Supplemental data for this article can be accessed here. https://doi.org/10.1080/21663831.2019.1604444

a self-trapped polaron level at oxygen vacancies to the valence band (VB). Due to disagreement and inconclusive identification on the origin of the blue emission band peaked at 2.8 eV, it appears relevant to tackle this puzzling scenario with an alternative strategy using *ion beam induced luminescence* or *ionoluminescence* (*IL*). Ion excitation has several key advantages over other excitation sources, which have not been, so far, sufficiently recognized: 1) it is a real-time *in-situ* technique with a very broad energy excitation spectrum in contrast to laser pulses; 2) it allows for an adjustable balance between the generation of point defects (associated mostly with elastic collisions) and electronic excitation, which can be modified through the choice of mass and energy of the incident ion; and 3) it has an easily adjustable excitation rate to investigate the role of electronic excitation density on the emissions.

2. Materials and methods

High-purity, epi-polished, stoichiometric $SrTiO_3$ (001) single crystals, provided by MTI Corporation Ltd., were irradiated in the Ion Beam Materials Laboratory (IBML UT-ORNL) at the University of Tennessee, Knoxville [31]. The irradiation setup along with the temperature control and the spectroscopic characterization have been described previously [21–23,32,33]. The relevant irradiation parameters, including electronic excitation densities and total number of oxygen vacancies generated per incident ion [34], are summarized in Table 1 (also Supplemental Material). Note that the electron–hole densities induced in this work are comparable to those induced in pulsed laser experiments.

3. Results and discussion

The 2.8 eV band is clearly enhanced relative to the 2.5 eV band with increasing excitation rate, a key finding of this work, when the emission spectra corresponding to irradiation with 8 MeV O and 18 MeV Cl ions are compared. Figure S2 (see supplementary data online) illustrates the representative emission spectra with several incident ions at low fluence ($\sim 10^{11}$ cm^{-2}) and different temperatures, together with the decomposition into three Gaussian bands, as previously described [21,22]. The above results appear similar to those obtained in $SrTiO_3$ under pulsed laser irradiation using different pulse energies [12], where it was found that the integrated light emission intensity grows linearly with excited carrier density up to around 5×10^{19} cm^{-3} (excitation density below 1 mJ/cm^2), where it starts reaching saturation.

The kinetics of the 2.8 eV band as a function of irradiation fluence offers new insights into the origin of this emission. Figure 1 illustrates the evolution of the 2.8 and 2.5 eV emission band yields under irradiation with several incident ions at different temperatures. The emission yield of the 2.8 eV blue band ($\boldsymbol{Y_B}$), as well as that for the 2.5 eV green band ($\boldsymbol{Y_G}$), rapidly increases with fluence (even though difficult to appreciate and evaluate in the figures) and reaches an essentially constant (steady-state) level after a fluence of $\approx 10^{11}$ cm^{-2}, typically associated with the establishment of a steady-state concentration of electron-holes (*e-h*) pairs. The initial evolution of such bands is considerably faster than that for the 2.0 eV band (not shown) confirming previously reported results [21–23] that associated this band to the generation of *isolated vacancies* during irradiation. The corresponding evolution of the emission yield for the green band is also shown in Figure 1 for comparison purposes. The similar evolution for both bands suggests a close correlation between them. In order to explore more quantitatively this correlation, Figure 2 plots the ratio, $\boldsymbol{\rho_{B/G} = Y_B/Y_G}$, between the integrated peak areas of the blue and green luminescence bands as a function of ion fluence at various temperatures. The ratio remains relatively constant as a function of fluence, with a small dispersion in the data of about 1% for lighter ions and 5-10% for the case of heavier ions and lower temperatures. These deviations can be expected due to heavy band overlap and the rapid evolution of the yields with fluence, especially at low temperatures. This figure confirms that $\boldsymbol{\rho_{B/G}}$ is independent of fluence at these temperatures. Moreover, this

Table 1. Irradiation parameters calculated using SRIM (version 2012) full-cascade simulations [34].

Ion, Energy (MeV)	R_p (μm)	$S_{e,max}$ (keV/nm)	E_{ioniz} (MeV)	F ($\times 10^{12}$ cm^{-2} s^{-1})	N_{e-h} ($\times 10^6$ e-h/ion)	G ($\times 10^{18}$ e-h cm^{-2} s^{-1})	$E_{recoils}$ (MeV)	Total Oxygen vacancies
H, 3	54.00	0.14	2.98	2.20	0.37	0.82	1.64×10^{-3}	11.42
O, 8	3.70	3.21	7.85	0.90	0.98	0.88	0.13	756.43
Si, 15	4.00	6.14	14.64	0.64	1.83	1.17	0.37	2002.95
Cl, 18	4.15	7.31	17.47	0.44	2.18	0.96	0.54	2816.96
Ti, 18	4.15	8.31	17.05	0.44	2.13	0.95	0.95	4749.95

R_p is the projected ion range, $S_{e,max}$ is the maximum electronic stopping power and E_{ioniz} stands for energy deposited into the electronic system per incident ion. F is the average irradiation flux. N_{e-h}, or *single-ion excitation rate g*, is the average number of *e-h* pairs generated by every single ion impact along R_p. G, the *overall electronic excitation rate*, represents the carrier *(e-h)* populations generated per unit time extended throughout R_p (see Supplemental Material). $E_{recoils}$ represents the total energy transferred per incident ion to target atoms (Sr, Ti and O) integrated along R_p, and *Total Oxygen vacancies* is the total number of oxygen vacancies produced per incident ion integrated along R_p.

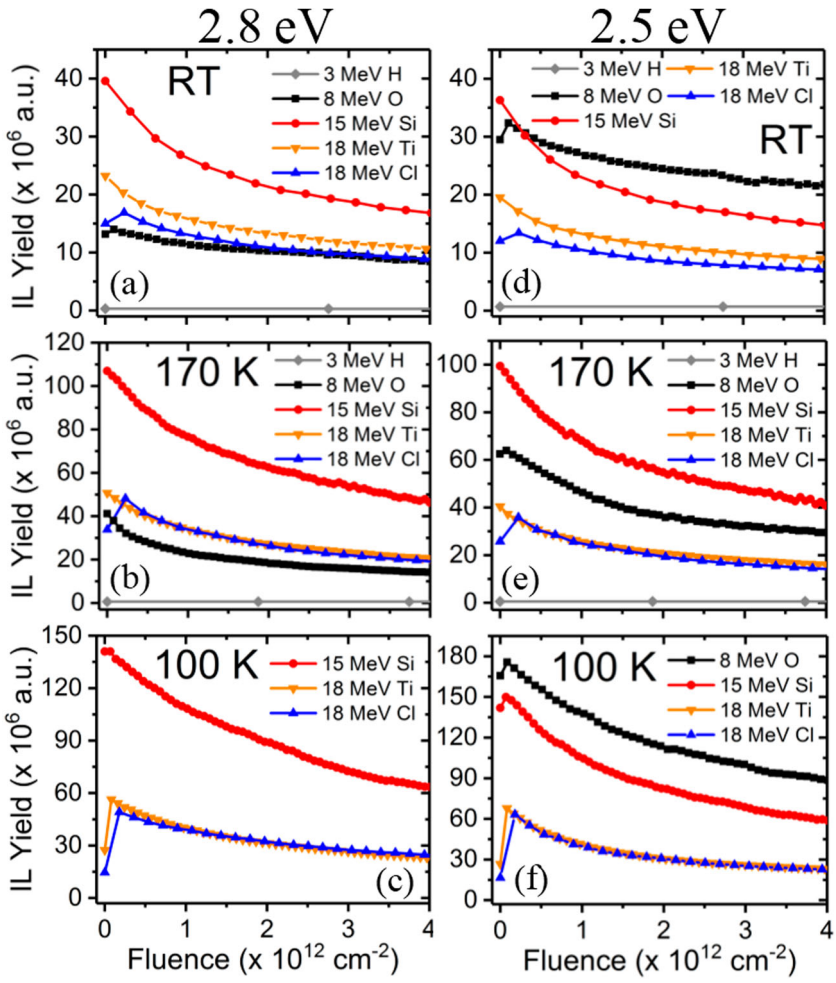

Figure 1. Kinetics of the emission bands at 2.8 eV (a-c) and 2.5 eV (d-f) as a function of ion fluence for different excitation rates (ions and energies) at different temperatures (RT, 170 and 100 K).

ratio $\rho_{B/G}$ clearly increases with the excitation rate, i.e. the 2.8 eV band is enhanced relative to the 2.5 eV band as the electronic excitation density increases, corroborating the case of laser pulse excitation [12–14].

Based on these novel results, we attribute the 2.8 eV band to optical transitions between CB levels and the localized STE ground state level. The CB levels become densely populated during the strong electronic excitation provided by heavy-mass and high energy ion-beam irradiation, which may account for a significant emission at 2.8 eV. This model states that both the blue and green bands are ascribed to transitions of the STE center, from either unbound (2.8 eV emission) or bound (2.5 eV emission) excited states, in accordance with the electronic levels scheme for all the optical transitions considered in Figure 3. The coexistence between these two types of transitions can only be achieved under high electronic excitation rates, such as those achieved by pulsed-laser or ion-beam irradiation. In accordance with this new model, the position of the *localized excited* STE level with respect to the CBM should match the difference between the energies of the blue (E_B) and green (E_G) emissions (leaving aside lattice relaxations), i.e. around 0.3–0.35 eV. On the other hand, the position of the *ground state* above the maximum of the VB for the two (green and blue) transitions would also be around E_B-$E_G \approx 0.35$ eV ($E_g \approx 3.25$ eV being the energy gap of $SrTiO_3$), suggesting a rather symmetrical position of the two STE levels inside the forbidden gap. Possible non-radiative Auger transitions that have been suggested by lifetime and integrated light intensity measurements for the 2.8 eV emission [12,17,18] are also indicated in Figure 3.

For a further quantitative interpretation of the kinetics, a definite model is needed. We assume that the main decay channel for the free carrier density is the formation of STEs through *bimolecular e-h* recombination followed by their associated green (2.5 eV) emission. Simultaneously, a *monomolecular* decay channel for free carriers to STEs levels accounts for the blue emission. We ignore any irradiation-induced defects, such as oxygen vacancies. This assumption is justified as long as the concentration of carriers, either electrons (*e*) or holes (*h*), is much

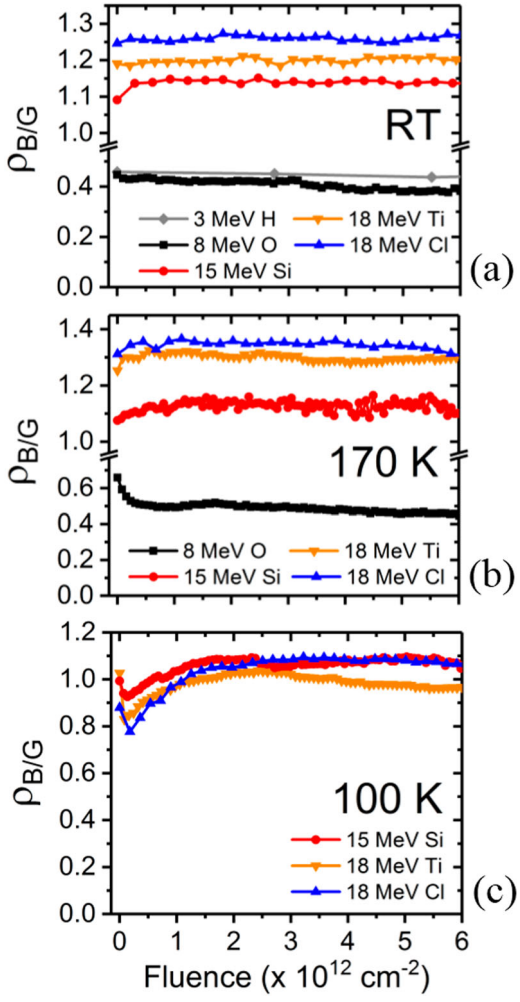

Figure 2. Evolution of the ratio ($\rho_{B/G}$) between the blue and green emission yields as a function of ion fluence for different excitation rates at different temperatures (RT, 170 and 100 K).

higher than that for defects. This is expected for sufficiently high *overall excitation rates* G, around or above 10^{20} cm^{-2} s^{-1}, comparable to those obtained under high power light pulses (see Table 1). This coexistence of *bimolecular* and *monomolecular* processes to account for the data on the emission lifetimes and yields as functions of excitation rate has been previously suggested by previous workers [13,14]. However, the strong overlap between the blue and green emission bands prevents quantitative separation of the two decay channels and the assignment of each to definite emissions (either green or blue). Previously reported data [13] on the photoluminescence spectra of pure and Nb-doped $SrTiO_3$, which showed a clear enhancement of the blue emission over the green one, are consistent with our current ion-beam results and the present model. Due to the electron donor character of Nb, the doped samples contain a much higher free electron concentration and, therefore, the corresponding blue emission for these samples

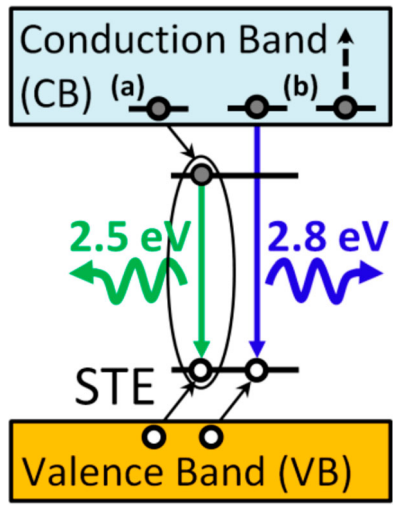

Figure 3. Proposed mechanisms for the main luminescence emissions at 2.5 eV and 2.8 eV. The blue (2.8 eV) and green (2.5 eV) luminescence emissions are, both, related to transitions of the STE center. (a) The radiative spontaneous annihilation of the STE is responsible for the green emission band. (b) The blue emission band is attributed to a radiative recombination of unbound states of the STE (i.e. free electrons in the CB) to the ground state level of the center. Possible alternative non-radiative channels for electronic Auger transitions to higher CB levels are indicated by dashed lines.

is strongly enhanced. For un-doped samples, a simple model, described below, predicts that the ratio, $\boldsymbol{\rho_{B/G}}$, between the two emission yields at 2.8 and 2.5 eV should evolve with the square-root of the excitation rate. For the *ion fluxes* considered in this work ($\sim 10^{11}$ cm^{-2} s^{-1}), the ion trajectories and subsequent excitation processes are essentially *uncoupled*, temporally and spatially, so that one can treat the effects of various incident ions as *independent events*. Therefore, in order to meaningfully compare the role of the different ions and energies on the ratio $\boldsymbol{\rho_{B/G}}$, one should use the excitation rate corresponding to a *single ion*, i.e. $g = N_{e-h}$ (see Table 1). This assumption is also reasonable given the fast dynamics (the lifetime, τ, for the 2.8 eV emission is on the nanosecond timescale) of the optical processes. In order to simulate the kinetics, one may proceed as follows: the evolution of the total carrier (e, h) and STE populations per *incident ion* in the irradiated volume, ignoring spatial variations along the ion projected range (R_p), can be described by the following rate equations:

$$\frac{dN_e}{dt} = \frac{dN_h}{dt} = g - \alpha N_e^2(t) \quad (1)$$

$$\frac{dN_{STE}}{dt} = \alpha N_e^2(t) - \beta N_{STE}(t) \quad (2)$$

with α being the recombination rate of carriers into STEs, β the light emission probability per unit of time

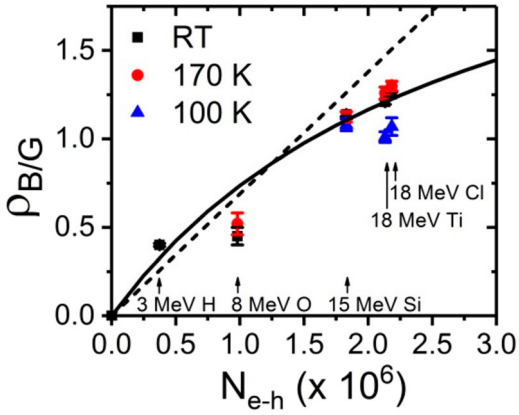

Figure 4. Dependence of $\rho_{B/G}$ on *single-ion excitation rate* (N_{e-h}) at different temperatures (RT, 170 and 100 K), revealing the sub-linear behavior on the excitation rate. Dots are averaged values extracted from data plotted in Figure 2 and the solid line corresponds to a square-root dependence. The dashed line represents a linear best fit.

(reciprocal of the STE lifetime, τ [9,10]), and $g = N_{e-h}$ the *excitation rate per incident ion*, extended throughout R_P. N_{e-h} values for the different ions are given in Table 1. The electron–hole (*e-h*) recombination rate, α, may be temperature dependent (through the electron–hole transport or tunneling processes to recombine into STEs). In the scale of the experiments under study, a steady state is rapidly reached:

$$N_{0,e} = \left(\frac{g}{\alpha}\right)^{\frac{1}{2}}, N_{0,STE} = \frac{g}{\beta} \tag{3}$$

Within this simple scheme, the overall yields for the green ($\boldsymbol{Y_G}$) and blue ($\boldsymbol{Y_B}$) emissions will be (ignoring possible self-absorption of the light):

$$Y_G \propto \beta N_{0,STE} \propto g \text{ (bimolecular channel)} \tag{4}$$

$$Y_B \propto N_{0,e} N_{STE} \propto g^{\frac{1}{2}} g \text{ (monomolecular channel)} \tag{5}$$

and the ratio between the yields is finally obtained as,

$$\rho_{B/G} = \frac{Y_B}{Y_G} \propto g^{\frac{1}{2}}. \tag{6}$$

Thus, at constant temperature the ratio should evolve with the excitation rate following a square-root dependence, as $g^{\frac{1}{2}}$. Figure 4 shows that the yields ratio $\boldsymbol{\rho_{B/G}}$ reasonably fits a square-root dependence on the *single-ion excitation rate*, N_{e-h}, which is consistent with the prediction of the above kinetic analysis. Therefore, the data confirms the physical model proposed for the STE and supports the assignment of the 2.8 eV emission to free carrier-STE recombination. One should remark that the situation under ion beam irradiation is not strictly equivalent to that under laser pulse excitation, since the individual photons are essentially coupled and cannot be separated in *space* or *time*.

4. Conclusion

In summary, a key result of the present study is that, the blue (2.8 eV) and green (2.5 eV) luminescence emissions are both related to transitions of the STE center, involving either localized states (2.5 eV), or pairs of localized and band states (2.8 eV). This represents a novel feature associated to the high electronic excitation densities achieved by both pulsed laser and ion beam irradiations. A new model for the blue emission is proposed consisting of a radiative transition from un-bound (CB) states to the ground STE level. Consequently, the two emissions (green and blue) are associated with the same localized center and imply the STE annihilation. The analysis presented here provides a unified description of the emission mechanisms and demonstrates the unique potential of ionoluminescence to unravel the rich and complex variety of effects associated with electronic carriers and oxygen vacancies in $SrTiO_3$.

Acknowledgments

This work was supported by the U.S. Department of Energy, Office of Science, Basic Energy Sciences, Materials Sciences and Engineering Division under Contract DE-AC05-00OR22725. M.L.C. and J.T.G. acknowledge support from the University of Tennessee Governor's Chair program.

Disclosure statement

No potential conflict of interest was reported by the authors.

Funding

This work was supported by the U.S. Department of Energy, Office of Science, Basic Energy Sciences, Materials Sciences and Engineering Division under Contract DE-AC05-00OR22725. M.L.C. and J.T.G. acknowledge support from the University of Tennessee Governor's Chair program.

ORCID

M. L. Crespillo http://orcid.org/0000-0001-5941-8426
Y. Zhang http://orcid.org/0000-0003-1833-3885
W. J. Weber http://orcid.org/0000-0002-9017-7365

References

[1] Reyren N, Thiel S, Caviglia AD, et al. Superconducting interfaces between insulating oxides. Science. 2007;317:1196–1199.
[2] Brinkman A, Huijben M, Van Zalk M, et al. Magnetic effects at the interface between non-magnetic oxides. Nature Mater. 2007;6:493–496.

[3] Wang D, Ye J, Kako T, et al. Photophysical and photocatalytic properties of $SrTiO_3$ doped with Cr cations on different sites. J Phys Chem B. 2006;110(32):15824–15830.
[4] Harrigan WL, Michaud SE, Lehuta KA, et al. Tunable electronic structure and surface defects in chromium-doped colloidal $SrTiO_{3-\delta}$ nanocrystals. Chem Mater. 2016;28(2):430–433.
[5] Ogale SB, editor. Thin films and heterostructures for oxide electronics. New York: Springer; 2005.
[6] Janotti A, Varley JB, Choi M, et al. Vacancies and small polarons in $SrTiO_3$. Phys Rev B. 2014;90:085202.
[7] Hao X, Wang Z, Schmid M, et al. Coexistence of trapped and free excess electrons in $SrTiO_3$. Phys Rev B. 2015;91:085204.
[8] Leonelli R, Brebner JL. Time-resolved spectroscopy of the visible emission band in strontium titanate. Phys Rev B. 1986;33(12):8649–8656.
[9] Hasegawa T, Shirai M, Tanaka K. Localizing nature of photo-excited states in $SrTiO_3$. J Lumin. 2000;87-89:1217–1219.
[10] Hasegawa T, Tanaka K. Photo-induced polaron states in strontium titanate. J Lumin. 2001;94-95:15–18.
[11] Kan D, Terashima T, Kanda R, et al. Blue-light emission at room temperature from Ar^+-irradiated $SrTiO_3$. Nature Mater. 2005;4:816–819.
[12] Yasuda H, Kanemitsu Y. Dynamics of non-linear blue photoluminescence and Auger recombination in $SrTiO_3$. Phys Rev B. 2008;77(19):193202.
[13] Rubano A, Ciccullo F, Paparo D, et al. Photoluminescence dynamics in strontium titanate. J Lumin. 2009;129:1923–1926.
[14] Rubano A, Paparo D, Miletto F, et al. Recombination kinetics of a dense electron-hole plasma in strontium titanate. Phys Rev B. 2007;76:125115.
[15] Rubano A, Paparo D, Radović M, et al. Time-resolved photoluminescence of n-doped $SrTiO_3$. Applied Phys Letters. 2008;92:021102.
[16] Rubano A, Paparo D, Miletto-Granozio F, et al. Blue luminescence of $SrTiO_3$ under intense optical excitation. J Appl Phys. 2009;106:103515.
[17] Yamada Y, Yasuda H, Tayagaki T, et al. Temperature dependence of photoluminescence spectra of non-doped and electron-doped $SrTiO_3$: crossover from Auger recombination to single carrier trapping. Phys Rev Lett. 2009;102:247401.
[18] Yamada Y, Kanemitsu Y. Band-edge luminescence from $STiO_3$: No polaron effect. Thin Solid Films. 2012;520(10):3843–3846.
[19] Aguilar M, Agulló-López F. X-ray induced processes in $SrTiO_3$. J Appl Phys. 1982;53:9009.
[20] Yang K-H, Chen T-Y, Ho N-J, et al. In-gap states in wide band gap $SrTiO_3$ analyzed by cathodoluminescence. J Am Ceram Soc. 2011;94(6):1811–1816.
[21] Crespillo ML, Graham JT, Agulló-López F, et al. Role of oxygen vacancies on light emission mechanisms in $SrTiO_3$ induced by high-energy particles. J Physics D: Appl Phys. 2017;50(15):155303.
[22] Crespillo ML, Graham JT, Agulló-López F, et al. Correlation between Cr^{3+} luminescence and vacancy disorder under MeV ion irradiation. J Phys Chem C. 2017;121(36):19758–19766.
[23] Crespillo ML, Graham JT, Agulló-López F, et al. Isolated oxygen vacancies in strontium titanate shine red: optical identification of Ti^{3+} polarons. Applied Materials Today. 2018;12C:131–137.
[24] Ricci D, Bano G, Pacchioni G, et al. Electronic structure of a neutral oxygen vacancy in $SrTiO_3$. Phys Rev B. 2003;68:224105.
[25] Hou Z, Terakura K. Defect states induced by oxygen vacancies in cubic $SrTiO_3$: First principles calculations. J Phys Soc Japan. 2010;79(11):114704.
[26] Mitra C, Lin C, Robertson J, et al. Electronic structure of oxygen vacancies in $SrTiO_3$ and $LaAlO_3$. Phys Rev B. 2012;86:155105.
[27] Alexandrov VE, Kotomin EA, Maier J, et al. First principles study of bulk and surface oxygen vacancies in STO_3 crystal. Eur Phys J B. 2009;72:53–57.
[28] Choi M, Oba F, Kumagai Y, et al. Anti-ferrodistortive-like oxygen-octahedron rotation induced by the oxygen vacancy in cubic $SrTiO_3$. Adv Mater. 2013;25(1):86–90.
[29] Leonelli R, Brebner JL. Evidence for bimolecular recombination in the luminescence spectra of $SrTiO_3$. Solid State Commun. 1985;54(6):505–507.
[30] Chen H, Umezawa N. Hole localization, migration and the formation of peroxide anion in perovskite $SrTiO_3$. Phys Rev B. 2014;90:035202.
[31] Zhang Y, Crespillo ML, Xue H, et al. New ion beam materials laboratory for effective investigation of materials modification and irradiation effects. Nucl Instrum Meth B. 2014;338:19–30.
[32] Crespillo ML, Graham JT, Zhang Y, et al. In-situ luminescence monitoring of ion-induced damage evolution in SiO_2 and Al_2O_3. J Lumin. 2016;172:208–218.
[33] Crespillo ML, Graham JT, Zhang Y, et al. Temperature measurements during high flux ion beam irradiations. Rev Sci Instrum. 2016;87(2):024902.
[34] Ziegler JF, Ziegler MD, Biersack JP. SRIM - The stopping and range of ions in matter. Nucl Instrum Methods B. 2010;268(11-12):1818–1823.